2013

Particulate Emissions Calculations from Fall Tillage Operations Using Point and Remote Sensors

Kori D. Moore
Utah State University, Kori.Moore@sdl.usu.edu

Michael D. Wojcik
Utah State University

Randal S. Martin
Utah State University

Christian C. Merchant
National Geospatial-Intelligence Agency

Gail E. Bingham
Utah State University

See next page for additional authors

Follow this and additional works at: http://digitalcommons.unl.edu/usdaarsfacpub

Authors

Kori D. Moore, Michael D. Wojcik, Randal S. Martin, Christian C. Merchant, Gail E. Bingham, Richard L. Pfeiffer, John H. Prueger, and Jerry L. Hatfield

Particulate Emissions Calculations from Fall Tillage Operations Using Point and Remote Sensors

Kori D. Moore,* Michael D. Wojcik, Randal S. Martin, Christian C. Marchant, Gail E. Bingham, Richard L. Pfeiffer, John H. Prueger, and Jerry L. Hatfield

Soil preparation for agricultural crops produces aerosols that may significantly contribute to seasonal atmospheric particulate matter (PM). Efforts to reduce PM emissions from tillage through a variety of conservation management practices (CMPs) have been made, but the reductions from many of these practices have not been measured in the field. A study was conducted in California's San Joaquin Valley to quantify emissions reductions from fall tillage CMP. Emissions were measured from conventional tillage methods and from a "combined operations" CMP, which combines several implements to reduce tractor passes. Measurements were made of soil moisture, bulk density, meteorological profiles, filter-based total suspended PM (TSP), concentrations of PM with an equivalent aerodynamic diameter ≤10 μm (PM_{10}) and PM with an equivalent aerodynamic diameter ≤2.5 μm ($PM_{2.5}$), and aerosol size distribution. A mass-calibrated, scanning, three-wavelength light detection and ranging (LIDAR) procedure estimated PM through a series of algorithms. Emissions were calculated via inverse modeling with mass concentration measurements and applying a mass balance to LIDAR data. Inverse modeling emission estimates were higher, often with statistically significant differences. Derived PM_{10} emissions for conventional operations generally agree with literature values. Sampling irregularities with a few filter-based samples prevented calculation of a complete set of emissions through inverse modeling; however, the LIDAR-based emissions dataset was complete. The CMP control effectiveness was calculated based on LIDAR-derived emissions to be 29 ± 2%, 60 ± 1%, and 25 ± 1% for $PM_{2.5}$, PM_{10}, and TSP size fractions, respectively. Implementation of this CMP provides an effective method for the reduction of PM emissions.

AGRICULTURAL AIR EMISSIONS of gaseous species and particles, such as ammonia (NH_3), volatile organic compounds, and particulate matter (PM), are being increasingly evaluated for their contributions to local and regional atmospheric loading and their effects on air quality. Sources of these emissions include animal husbandry, waste management, harvesting, and tillage operations. The USEPA has set National Ambient Air Quality Standards (NAAQS) for ambient concentrations of designated criteria pollutants (CO, NO_x, O_3, SO_x, particulate matter with an equivalent aerodynamic diameter ≤10 μm [PM_{10}] and particulate matter with an equivalent aerodynamic diameter ≤2.5 μm [$PM_{2.5}$], and Pb). Air quality regulatory agencies use the NAAQS to regulate emissions of pollutants that contribute to the concentration of criteria pollutants, with more stringent emissions requirements in areas determined to be in "nonattainment" with the NAAQS.

The San Joaquin Valley Air Basin was classified as being in nonattainment for PM_{10} until November 2008. As such, the San Joaquin Valley Air Pollution Control District (SJVAPCD) was required to implement emission controls for all significant PM_{10} sources to reduce primary PM_{10} emissions. Agricultural operations above a specified size that grow crops and/or have animal feeding operations were included in the list of significant sources required to reduce emissions and subjected to SJVAPCD Rule 4550, Conservation Management Practices (CMPs), passed in August 2004. To meet targeted PM emissions reductions, producers were required to choose at least one CMP from a list of several options for each applicable management area, submit the planned CMP strategy, and implement it once the plan was approved. The small amount of data available in the literature

K.D. Moore, M.D. Wojcik, and G.E. Bingham, Space Dynamics Laboratory, Utah State Univ. Research Foundation, 1695 N. Research Park Way, N. Logan, UT 84341; R.S. Martin, Dep. of Civil and Environmental Engineering, Utah State Univ., 4110 Old Main Hill, Logan, UT 84322; C.C. Marchant, National Geospatial-Intelligence Agency, 7500 Geoint Drive, Springfield, VA 22150; R.L. Pfeiffer, J.H. Prueger, and J.L. Hatfield, National Laboratory for Agriculture and the Environment, Agricultural Research Service, U.S. Department of Agriculture, 2110 University Boulevard, Ames, IA 50011. Assigned to Associate Editor Barbara Amon.

Abbreviations: AERMOD, The American Meteorological Society and USEPA regulatory model; agl, above ground level; CI, confidence interval; CMP, conservation management practice; EF, emission factor; ER, emission rate; LIDAR, light detection and ranging; MCF, mass conversion factor; NAAQS, National Ambient Air Quality Standards; OPC, optical particle counter; PM, particulate matter; $PM_{2.5}$, particulate matter with an equivalent aerodynamic diameter ≤2.5 μm; PM_{10}, particulate matter with an equivalent aerodynamic diameter ≤10 μm; TSP, total suspended particulate (particulate matter with an equivalent aerodynamic diameter ≤100 μm).

concerning the variety of CMPs for tillage activities required that most control efficiencies were estimated from emissions measurements of other operations (SJVAPCD, 2006). Although the San Joaquin Valley Air Basin is classified as in attainment with the PM_{10} NAAQS, its maintenance plan requires the same strategies used to bring it back into attainment continue to be applied. In addition, other PM_{10} nonattainment areas, such as Imperial Valley, California and Phoenix, Arizona, have CMP or best management practice rules in place for agricultural tillage practices.

Previous research on PM emissions from agricultural tillage operations (Holmen et al., 1998, 2001a, 2001b; Flocchini et al., 2001; Madden et al., 2008; Wang et al., 2010; Kasumba et al., 2011) have focused almost exclusively on PM_{10} emission rates (ERs) and emission factors (EFs). A significant conclusion from Flocchini et al. (2001) found that emission factors were significantly influenced by environmental conditions (e.g., near-ground temperature profile, relative humidity, and soil moisture), and the potential variability of emissions from the same implement under opposing extreme environmental conditions may be larger than the variation from the type of crop or equipment used for tilling. Holmen et al. (1998) used elastic LIDAR (light detection and ranging) data collected during tillage emissions measurements to track plume movements in the downwind vertical plane and demonstrated that plume depths were greater than the elevated point sensors located downwind at 10 m above ground level (agl). They suggested the best method for sampling fugitive dust includes a combination of elastic LIDAR and strategically placed point samplers. Marchant et al. (2011) used point sensors and a mass calibrated LIDAR to investigate fugitive dust emissions from a dairy. Madden et al. (2008) is the only one to report PM_{10} emissions from standard tillage operations and a CMP (strip-till). The California Air Resource Board (ARB) developed area source PM_{10} emission inventory calculation methodologies for agricultural tillage and harvesting operations based on the report by Flocchini et al. (California ARB, 2003a, 2003b).

A Regional Applied Research Effort grant was awarded to the USEPA Office of Research and Development, National Exposure Research Laboratory to investigate the control effectiveness of one or more of the listed SJVAPCD CMPs using advanced measurement technologies in a field-scale setting. This study was designed to address the following research questions:

(i) What are the magnitude, flux, and transport of PM emissions produced by agricultural practices for row crops where tillage CMPs are being implemented versus the magnitude, flux, and transport of PM emissions produced by agricultural practices where CMPs are not being implemented? (ii) What are the control efficiencies of equipment being used to implement the "combined operations" CMP? and (iii) Can these CMPs for a specific crop be quantitatively compared, controlling for soil type, soil moisture, and meteorological conditions? The main focus of this research was to quantify the control effectiveness of the selected CMP, which required the emissions to be quantified, and it was not an effort to provide representative emission factors for any one of the agricultural operations involved. This paper summarizes the results of the PM measurements made during a field experiment and the calculated ERs and addresses these research questions. A full report detailing all of the sampling methodology and results is given in Williams et al. (2012).

Materials and Methods

The fall tillage sequence after harvest of a row crop (cotton) was selected for this comparison study. The experiment was performed near Los Banos, California, during October 2007 on two adjacent fields with nearly identical crop and irrigation treatment over the previous several years. Both fields were planted in cotton for the 2007 growing season, which had been harvested before tillage activities with the stalks shredded and left on the ground (cooperating producer, personal communication, 2007). The site was chosen based on producer cooperation, historically dominant northwest winds, and field layout. The surrounding landscape was flat and dominated by agricultural crop production. Soil survey data from the USDA-NRCS list the soil in both fields as being dominated by nearly identical distributions of three clay loam classifications (103: Alros clay loam, partially drained; 139: Bolfar clay loam, partially drained; and 170: Dos Palos clay loam, partially drained) (Soil Survey Staff, 2007).

The CMP selected for investigation was the combined operations method, which reduces the number of passes by combining multiple operations into one. The CMP implement used was the Optimizer 5000 (Tillage Management), which incorporates all forms of conventional tillage into a single pass. The CMP was applied to Field B (51.8 ha), and standard practices were used in Field A (25.5 ha). The sampling schedule is given in Table 1, providing the date, operation, sample time, total tractor

Table 1. Sample schedule and sample period tillage and meteorological characteristics. Meteorological parameters measured at 5 m above ground level.

Date	Tillage operation	Sample time	Total tractor time	Total area tilled	Tillage rate	Mean temp. $\pm 1\sigma$	Mean wind speed $\pm 1\sigma$	Mean wind direction $\pm 1\sigma$
		h	$h_{tractor}$	ha	ha $hr_{tractor}^{-1}$	°C	m s^{-1}	°
			Combined operations practice—Field B					
19 Oct.	Chisel	5.33	8.5	22.0	2.6	20.5 ± 2.8	1.1 ± 0.3	43 ± 62
20 Oct.	Optimizer	2.85	4.36	20.0	4.7	16.8 ± 1.3	6.9 ± 2.0	320 ± 1
			Conventional practice—Field A					
23 Oct.	Disc 1	7.27	11.0	24.8	2.3	26.1 ± 2.6	1.6 ± 0.6	320 ± 7
25 Oct.	Chisel	4.24	6.5	19.5	3.0	27.4 ± 1.8	1.2 ± 0.8	338 ± 9
26 Oct.	Disc 2A	5.52	3.4	10.5	3.0	22.0 ± 1.9	2.9 ± 0.8	328 ± 5
27 Oct.	Disc 2B	4.09	5.75	14.2	2.5	22.7 ± 1.9	3.1 ± 1.3	10 ± 33
	Total Disc 2	9.61	9.16	24.7	2.7	–	–	–
29 Oct.	Land plane	3.49	3.33	8.0	2.4	23.5 ± 1.6	1.7 ± 0.9	1 ± 19

time, total area tilled, and tillage rate. Most of the operations had two tractor and implement pairs working the field at one time; total tractor time is the sum of time spent by each tractor and implement pair tilling the field. Less than the full field was tilled in each measurement period due to environmental, temporal, and equipment factors. For example, there were two samples collected for the Disc 2 pass; farm equipment malfunctions during the Disc 2A sample period halted the operation, and it was resumed the following day when the remainder of the field was tilled in the Disc 2B sample period.

Sample Layout

Sensors for PM and meteorology were distributed to measure upwind and downwind conditions based on the historically dominant northwest wind. Meteorological characterizations were performed at upwind, downwind, and crosswind locations with the instrumentation described in Table 2. Vertical temperature, humidity, and wind speed profiles were measured using two 15.3-m towers, one upwind and one downwind as shown in Fig. 1. Each tower had five humidity/temperature sensors at 1.5, 2.5, 3.9, 6.2, and 9.7 m agl and three-cup anemometers at 2.5, 3.9, 6.2, 9.7, and 15.3 m agl. Wind direction was measured at 15.3 m using a wind vane. Wind direction measurements were made at 15.3 m agl on the towers instead of 10 m, as is typical, because LIDAR measurements were made at higher elevations (up to 200 m agl) and because the 15.3-m measurement height was reasoned to provide a better representation of ground level and higher elevation wind direction than the 10 m height. A meteorological station monitored wind speed, wind direction, temperature, relative humidity, precipitation, barometric pressure, and solar radiation at 5 m agl at the air quality trailer locations shown in Fig. 1. Four pairs of three-dimensional sonic anemometers and infrared gas analyzers were deployed around the fields to characterize upwind and downwind turbulence, as well as vertical fluxes of latent heat (evaporation), sensible heat, carbon dioxide, and horizontal momentum. Bulk density and soil moisture were quantified before each operation, with calculations performed as described in Doran and Jones (1996).

Particulate matter was characterized by 30 MiniVol Portable Air Samplers (AirMetrics), a filter-based mass concentration sampler, and by nine Aerosol Profilers (model 9722, Met One Instruments), also known as optical particle counters (OPCs). The MiniVol is a portable, programmable, filter-based sampler that yields mass concentration averaged over the sample time, with an impactor plate assembly used for a single-sized particle fractionation for $PM_{2.5}$, PM_{10}, and TSP. MiniVol flow calibration was performed before deployment. Pre- and postweights for the 47-mm Teflon filters used in the MiniVols were quantified using a calibrated microbalance (Type MT5, Mettler-Toledo, Inc.) at the Utah Water Research Laboratory in Logan, Utah. Filter conditioning was performed in accordance with guidance in 40 CFR 50 Appendix J (USEPA, 1987). The OPCs sum particle counts in eight size bins over nominal 20-s sample periods with lower bin limits of 0.3, 0.5, 0.6, 1.0, 2.0, 2.5, 5.0, and 10.0 μm; the last channel counts particles >10.0 μm. Optical particle counter flow and count calibrations were performed on site and applied in postanalysis. These instruments were deployed in a sampling array surrounding the field of interest at 2 and 9 m agl. At most of the locations, multiple MiniVols with different size–fractionation configurations and an OPC were collocated to characterize particle size and mass distributions.

Particle volume concentrations (V_k) for each size fraction (k) were calculated from OPC particle counts assuming a spherical shape. MiniVol-measured mass concentrations in each size fraction (PM_k) were divided by the corresponding period-averaged V_k on a location-by-location basis. This ratio was termed a "mass conversion factor" (MCF) by Zavyalov et al. (2009) and is a simple scalar representation of a complex and varying relationship between optical and aerodynamic measurements. It incorporates many factors, such as particle shape, porosity, density, indices of refraction different from OPC calibration aerosols, and instrument sampling efficiencies, into a single value. Average MCFs were calculated across sampling locations for each size fraction on each day.

In addition to the point sensors, the Aglite LIDAR system was used in characterizing particulate emissions from each tillage activity. The Aglite LIDAR is a portable system using a

Table 2. Manufacturer, precision, and accuracy information for deployed meteorological instrumentation.

| Instrument model	Manufacturer	Measured parameter	Accuracy
HMP45C	Vaisala, Oulu, Finland	temperature	±0.2°C at 20°C
		relative humidity	±2% for values in the 0–90% range and ±3% for values in the 90–100% range
Gill 3-cup anemometer	RM Young Co., Traverse City, MI	horizontal wind speed	±0.2 m s^{-1} over 1 m s^{-1}; threshold speed = 0.5 m s^{-1}
024A Wind Vane	Met One Instruments, Grants Pass, OR	wind direction	±5°
Vantage Pro2 Plus Weather Station	Davis Instruments, Inc., Hayward, CA	temperature	±0.5°C for values greater than −7°C; ±1.0°C for values less than −7°C
		relative humidity	±3% for values 0–90% and ±4% for values 90–100%
		horizontal wind speed	±1 m s^{-1} or 5%, whichever is greater
		wind direction	±3°
		precipitation	±3% or 0.02 mm per event, whichever is greater
		barometric pressure	±0.8 mm Hg at 25°C
		solar radiation	±5% of full scale
CSAT	Campbell Scientific, Inc., Logan, UT	three-dimensional wind vector	offset error less than ±8 cm s^{-1}; gain error for wind vector within 20° of horizontal less than ±6% of reading
7500 Infrared Gas Analyzer	LI-COR, Lincoln, NE	gaseous H_2O and CO_2 concentrations	dependent on calibration and environmental conditions
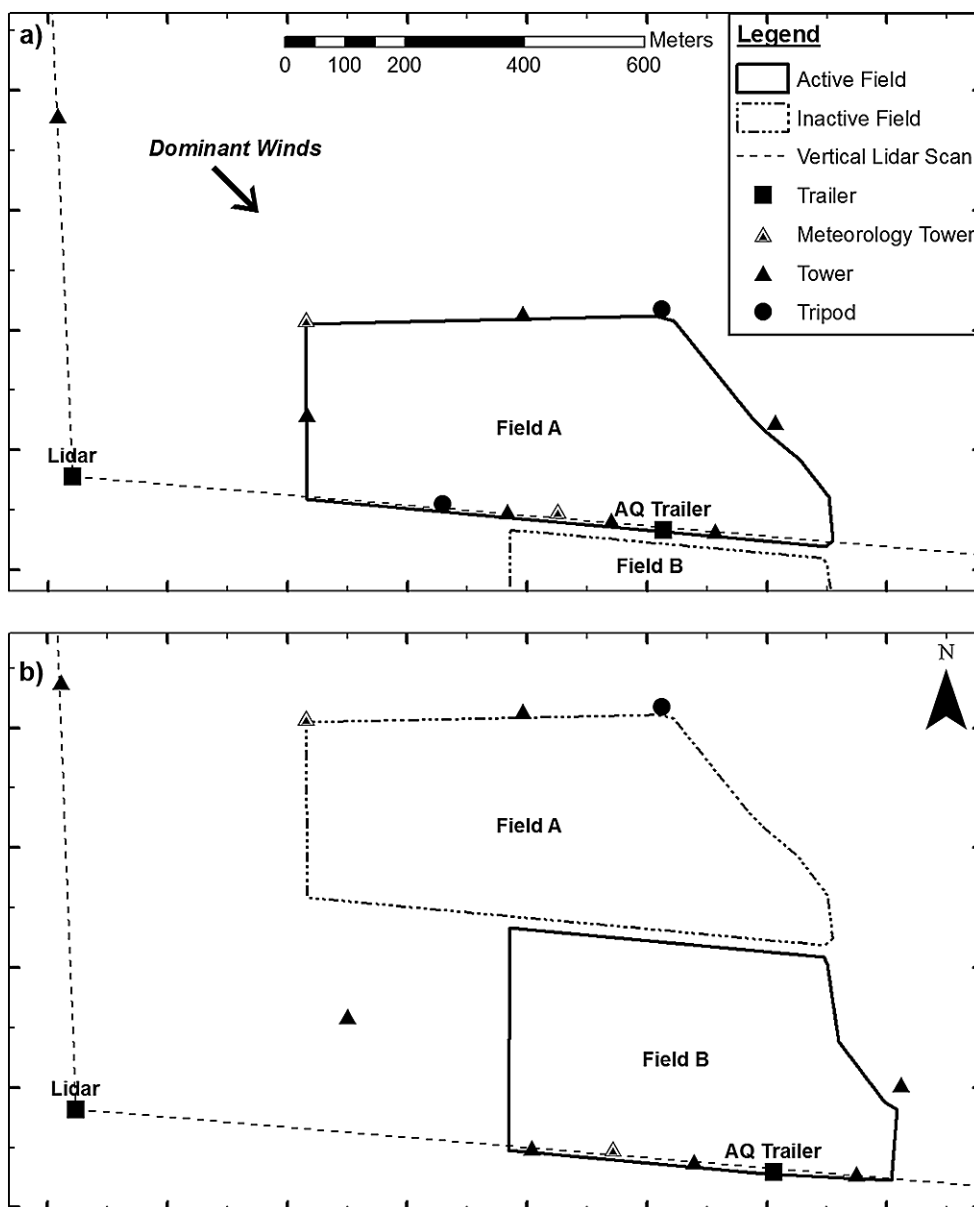
Fig. 1. Sample layouts for particulate matter and meteorological measurements made during (a) conventional tillage operations in Field A and (b) the combined operations conservation management practice operations in Field B. AQ, air quality.

micro-pulsed Nd:YAG laser with three wavelengths (355, 532, and 1064 nm) with the capability to scan 280° in azimuth and from −5° to +40° in elevation. The effective range is 500 m to 15 km, with a range bin size of 6 m. The Aglite LIDAR was placed in a crosswind position ≥400 m away from the nearest tillage area border. It continuously performed vertical scans on the upwind and downwind sides of the field, horizontal scans over the field, and calibration stares throughout tillage observation periods. A calibration stare refers to short periods (60–120 s) when the LIDAR beam is held adjacent to the upwind calibration tower, which is instrumented with collocated OPC and MiniVols; calibration stares were performed routinely throughout the sample period at 15- to 20-min intervals. In postprocessing, LIDAR return signals were calibrated to particle size distribution and particle volume concentrations based on upwind calibration stares through Klett's inversion (Marchant et al., 2009). Conversion from particle volume concentration

to mass concentration was accomplished with MCFs. This calibration method converts LIDAR data points along the beam path to mass concentration, which allows a scanning LIDAR to estimate PM concentrations in the volume of air surrounding an area of interest. Detailed descriptions of the LIDAR system, inversion technique, and data analysis are provided by Marchant et al. (2009) and Zavyalov et al. (2009).

Emission Calculation Methods

The ERs and EFs were calculated using two different methods from the collected filter and LIDAR data to estimate the control efficiency of the combined operations CMP in this study. The $PM_{2.5}$, PM_{10}, and TSP concentrations measured by the MiniVols were coupled with an air dispersion model through inverse modeling. In inverse modeling, the measured concentration attributable to the activity is known (measured downwind concentrations minus upwind/background concentrations), but

the ER is unknown. The ER supplied to the model is adjusted to best match the modeled concentrations to the measured contributions from the activity. AERMOD, the current USEPA-recommended steady state-air dispersion model, was used to perform the inverse modeling estimation of observed emission rates through AERMOD View, a commercially available user interface from Lakes Environmental, Inc., with AERMOD version 07026. On-site measured wind speed, wind direction, temperature, humidity, and solar radiation were used by AERMET, the meteorological preprocessor for AERMOD, to create surface and elevated meteorological input files. Percent cloud cover was set to zero based on visual observations during the measurement periods, and default agricultural land autumn values of noon-time albedo (0.18) and surface roughness length (0.05 m) were selected. A Bowen ratio value of 1.0 was used instead of the default autumn value of 0.7 due to the dry, bare soil surface. Tillage areas and sampler locations were measured by a hand-held GPS unit and included as AERMOD inputs. Modeled plume edge effects on the ER were avoided by eliminating locations with modeled concentrations less than 10% of the maximum modeled concentration from calculations, as per Arya (1998).

The second ER and EF calculation approach was a mass balance applied to the mass concentration-calibrated LIDAR data. Assuming uniform background aerosol levels, average upwind concentrations were subtracted from concentrations in and around detected plumes in the downwind vertical scans. The difference was multiplied by the component of the minute-averaged wind perpendicular to the beam, which is a function of elevation, to calculate the horizontal flux of PM through the vertical plane. Fluxes were summed across the vertical plane, averaged over the length of the sample period, and then divided by the size of the tilled area to calculate the mean EF of PM from the field surface. The EF was further divided by the total tractor time to calculate the mean ER of each operation. This method of calculating ERs and EFs using LIDAR is provided in detail in Bingham et al. (2009).

Vertical wind speed profiles up to 250 m agl were calculated to estimate the horizontal flux of PM through the downwind vertical LIDAR scanning plane, though most sample periods did not require data more than 150 m agl. Profiles were developed using cup anemometer measurements from the tower in the northwest corner of Field A and the following power law, as given by Cooper and Alley (2002).

$$u_2 = u_1 \left(\frac{z_2}{z_1} \right)^p$$

where z_1 is the lower elevation with units of m; z_2 is the higher elevation in m; u_1 and u_2 are the wind speeds in m s^{-1} at the lower and higher elevations, respectively; and p is a dimensionless number that varies with atmospheric stability. Cooper and Alley list $p \approx 0.5$ for very stable conditions and $p \approx 0.15$ for very unstable conditions. Values of p used to calculate vertical profiles were estimated by solving the above equation for p and using average wind speeds, nominally from the 2.5 and 9.7 m measurement elevations. Estimated period-average p values ranged between 0.16 and 0.22 and averaged 0.20. Vertical profiles were calculated with u_1 values taken from measurements at z_1 = 9.7 m.

Wind direction over the vertical profile was assumed to be constant. Although wind direction is known to change in a vertical profile, the influencing factors may be complex and the magnitude and direction of change highly variable. Therefore, in the absence of measured data, the assumption that wind direction did not change with increasing elevation over the 250-m profile was used. Wind direction as measured by the sonic anemometer on the northwest corner of Field A at 11.3 m agl was used for these analyses.

Results and Discussion

Observed wind conditions throughout the field study were very similar to the conditions observed during the month of October for previous years at Station #56 of the California Irrigation Management Information System (CIMIS) located near Los Banos, California, with dominant winds from the northwest. Mean temperature, wind speed, and wind direction values ±1σ for each sample period are given in Table 1. Unfortunately, light and variable winds delayed and/or affected sampling on several occasions; one example of an affected period is the 19 October sample period, which had an average wind speed of 1.1 m s^{-1} and a high wind direction SD of 62°. In addition, two precipitation events were recorded immediately before the first sample period and one between the last two sample periods that affected soil surface conditions. Evapotranspiration calculations from the downwind latent heat flux measurements suggested that no residual water was present in the soil from precipitation events before the first sample period. However, it did suggest that residual water was present in the soil during the last sample period (land plane operation) from the rainfall 2 d prior.

Soil bulk densities measured in the furrows and ridges averaged ±1σ 1.47 ± 0.02 g cm^{-3} and 1.37 ± 0.03 g cm^{-3}, respectively, for Field B (combined operations CMP treatment) and 1.52 ± 0.06 and 1.34 ± 0.05 g cm^{-3}, respectively, for Field A (traditional treatment). Higher average soil moisture conditions ±1σ were present in furrows at 10.3 ± 0.49% for Field B and 11.34 ± 0.61% for Field A, whereas the ridges were drier at 9.45 ± 0.06% and 8.08 ± 0.08% for Fields B and A, respectively. Soil moisture was highest in both fields before any tillage activity and decreased as the number of tillage operations increased.

MiniVol sampler–measured PM$_{2.5}$ concentrations ranged from 5.8 to 52.9 µg m^{-3}, PM$_{10}$ concentrations ranged from 16.3 to 165.3 µg m^{-3}, and TSP concentrations ranged from 60.5 to 203.3 µg m^{-3}. Filter samples were passed through a rigorous QA/QC process that included examination of the filters during handling of sampler-run data and of calculated concentrations to identify potential data outliers. Only filters that passed QA/QC were used in emissions calculations.

Time-series OPC data were used to examine potential impacts on upwind samplers. The majority of observed impacts on upwind samples were due to unpaved road traffic associated with logistical support for the tillage operations. However, significantly elevated PM levels of short duration were detected during a few periods of variable wind conditions and an absence of nearby unpaved road traffic. These anomalies are likely due

to tillage plumes from the field under study being transported to upwind sample locations. Most of the affected upwind samples were removed from further calculations. However, there were three sample periods in which nonaffected background samples did not exist. In these instances, background PM levels for emission calculation purposes were estimated through multiplication of the affected MiniVol concentration by a ratio of OPC V_k data (average V_k excluding time periods with impacts divided by the period-average V_k). The assumption is that this ratio would remain constant between volume and mass concentration and is based on similar chemical compositions between the background and plume aerosols, as shown in chemical analyses performed on collected particulates (not reported herein) and supported by similar MCFs calculated across all sites. These OPC V_k ratios averaged $\pm 1\sigma$ 0.98 ± 0.02 for $PM_{2.5}$, 0.82 ± 0.12 for PM_{10}, and 0.84 ± 0.13 for TSP over the three sample periods.

Period-average MCFs for the $PM_{2.5}$ size fraction ranged from 2.16 to 4.90 g cm^{-3}, with a mean $\pm 1\sigma$ of 2.95 ± 1.25 g cm^{-3}. Mass conversion factors for the PM_{10} size fraction had a mean of 1.44 ± 0.44 g cm^{-3} with a range of 1.29 to 1.71 g cm^{-3}, and TSP MCFs ranged from 0.63 to 2.77 g cm^{-3} with a mean of 1.53 ± 0.90 g cm^{-3}. Day-to-day variation in the MCF is not fully understood but is likely due to changes in background aerosol sources and composition because the point samplers collected ambient aerosol for a much larger period of time than the nonstationary tillage plume. The LIDAR and OPC data were converted from particle volume concentration to particle mass concentration using the sample period average MCF values.

Comparisons of PM levels measured or estimated by collocated MiniVols, OPCs, and the LIDAR bin adjacent to the tower were made at upwind and downwind elevated locations to verify estimated LIDAR and OPC PM concentrations. An example of these comparisons is presented in Table 3. As can be seen in this example, the calculated concentrations agree fairly well for $PM_{2.5}$ and TSP at the upwind location, although upwind PM_{10} LIDAR levels were 130% of the adjacent MiniVol sampler concentrations and 85% of the adjacent OPC values. Reported downwind concentrations were significantly different at all size fractions, with the LIDAR greater than the adjacent PM sampler by 421, 257, and 147% for $PM_{2.5}$, PM_{10}, and TSP, respectively, and greater than the

adjacent OPC by 326, 305, and 307% for $PM_{2.5}$, PM_{10}, and TSP, respectively. Differences, particularly in downwind values, may be attributed to several factors, including sample volume differences (OPCs: 1 L min^{-1}; MiniVols: 5 L min^{-1}; LIDAR: 6 m bin length × ~1 m beam diameter sampled at 10 kHz with data averaged over 0.5 s), sampling frequency at the comparison location (MiniVol and OPC: continuous; LIDAR upwind: ~2 min per 15 min; and LIDAR downwind: ~10 s per 15 min), LIDAR sample timing/frequency with respect to plume location (i.e., simultaneous presence of the LIDAR beam and transient plume in the bin of interest adjacent to the tower versus the total time the plume affected the instrumented tower), and the differences between the MCF values calculated at the comparison site and the average MCF across all measurement sites used to convert OPC and LIDAR particle volume concentrations to mass concentration.

Emissions Calculations

The average MiniVol-measured upwind PM concentrations were subtracted from the individual downwind concentrations to determine the impact of the operation on measured PM. Only downwind samples with levels greater than the average upwind concentration plus the corresponding 67% confidence interval (CI), selected to correspond with 1 SD away from the mean, were used in emissions calculations. This statistical difference was not achieved by any downwind $PM_{2.5}$ measurements from two sample periods: the chisel pass of the combined operations treatment (19 Oct.) and the Disc 1 pass of the traditional treatment (23 Oct.). Therefore, no $PM_{2.5}$ emissions based on inverse modeling were calculated for these operations. Only two downwind PM_{10} samples passed this statistical comparison from the chisel pass of the traditional tillage treatment on 25 October, and statistical measures about the mean were omitted for that period.

A ratio of the measured over the modeled impact at each location with valid measured values was calculated and averaged across all locations. The average ratio is the required scalar adjustment to the initial ER provided to the dispersion model to yield an average measured-over-modeled ratio of 1.0, which then becomes the estimated ER for that operation. This method was applied to all size fractions with statistically significant measured differences between upwind and downwind for all tillage

Table 3. Comparison of average particulate matter mass concentrations with respective 95% confidence intervals about the mean as reported by collocated MiniVol particulate matter samplers, optical particle counters, and light detection and ranging at an upwind and downwind location for the 23 October sample period.

Measured concentrations†	$PM_{2.5}$	PM_{10}	TSP
	——————— μg m^{-3} ———————		
Upwind			
PM sampler	17.0	35.9	60.5
Upwind PM sampler average ± 95% CI	16.1 ± 1.2	39.6 ± 7.2	60.5
OPC ± 95% CI	13.9 ± 0.2	54.5 ± 3.9	65.6 ± 6.3
LIDAR ± 95% CI	13.8 ± 0.2	45.9 ± 0.9	60.1 ± 1.4
Downwind			
PM sampler	9.9	75.5	203.3
Downwind PM sampler average ± 95% CI	11.8 ± 2.5	59.7 ± 8.4	203.3
OPC ± 95% CI	12.8 ± 0.2	63.5 ± 3.1	97.0 ± 13.0
LIDAR ± 95% CI	41.7 ± 9.0	193.7 ± 47.7	297.7 ± 76.6

† CI, confidence interval; LIDAR, light detection and ranging; OPC, optical particle counter; PM, particulate matter.

operations using the AERMOD dispersion model. Average estimated ER values, in units of mass per unit area per unit time, for each operation are listed in Table 4. Emission factors in units of mass per unit area tilled were calculated by multiplying the ERs by total tillage time and are listed in Table 5.

The $PM_{2.5}$ and PM_{10} ERs and EFs for the Disc 2 pass are averages over two sample periods (26 and 27 Oct.). Tillage equipment malfunctions on 26 October delayed completion of the operation until the following day. Additionally, due to the absence of a valid downwind TSP sample for 26 October and the model-predicted concentration at the downwind TSP sample location being about 7% of the maximum predicted concentration on 27 October, the TSP EF for the Disc 2 pass was calculated by assuming that the PM_{10}/TSP EF ratio observed during the Disc 1 pass of 0.12 was representative of disc passes under similar conditions and then dividing the Disc 2 PM_{10} EF of 149.2 mg m^{-2} by 0.12 to yield a TSP EF of 1210.0 mg m^{-2} for the operation.

Emissions from LIDAR measurements were estimated using a simple mass balance technique. Average flux values for each tillage operation were calculated, multiplied by total tillage time, and divided by total area tilled to yield EF values in mass per unit area tilled. These are presented in Table 5 with their associated 95% CIs. The EFs were then divided by total tractor time to yield ERs in mass per unit area tilled per unit time of operation and are given in Table 4. The reported Disc 2 ERs/EFs are weighted averages of the two sample periods, with the weights calculated

Table 4. Mean emissions rates and 95% confidence intervals calculated using inverse modeling with AERMOD and filter-based particulate matter measurements and the mass balance technique applied to particulate matter–calibrated light detection and ranging data.

Operation	$PM_{2.5}$ ER†		PM_{10} ER		TSP ER	
	AERMOD	LIDAR	AERMOD	LIDAR	AERMOD	LIDAR
			μg s^{-1} m^{-2}			
			Combined operations CMP‡ method			
Chisel	–	1.5 ± 0.4	5.2 ± 4.6***	2.3 ± 0.7***	9.1	8.7 ± 2.5
Optimizer	4.5 ± 7.0***	2.1 ± 0.3***	6.6 ± 7.7***	2.7 ± 0.4***	24.6	10.8 ± 1.7
			Conventional method			
Disc 1	–	0.5 ± 0.1	3.2 ± 1.5***	2.5 ± 0.3***	25.7	4.0 ± 0.5
Chisel	1.5 ± 4.9 ns§	1.5 ± 0.3 ns	7.2	3.4 ± 0.6	18.1	10.0 ± 1.7
Disc 2	0.7 ± 0.2***	1.2 ± 0.3***	4.5 ± 2.8***	2.4 ± 0.6***	36.7	4.5 ± 1.2
Land plane	1.5	1.2 ± 0.3	3.4 ± 0.9***	1.8 ± 0.5***	3.2	2.8 ± 0.8

*** Difference between emission calculation methods is significant at the 0.001 probability level.

† ER, emission rate; LIDAR, light detection and ranging; $PM_{2.5}$, particulate matter with an equivalent aerodynamic diameter ≤2.5 μm; PM_{10}, particulate matter with an equivalent aerodynamic diameter ≤10 μm; TSP, total suspended particulate (particulate matter with an equivalent aerodynamic diameter ≤100 μm).

‡ Conservation management practice.

§ Nonsignificant at the 0.20 probability level.

Table 5. Mean emission factors and 95% confidence intervals calculated via inverse modeling with AERMOD and filter-based particulate matter measurements and the mass balance technique with particulate matter–calibrated lidar data for each operation, as well as the calculated control efficiencies of the combined operations conservation management practice method.

Operation	$PM_{2.5}$ EF†		PM_{10} EF		TSP EF	
	AERMOD	LIDAR	AERMOD	LIDAR	AERMOD	LIDAR
			mg m^{-2}			
			Combined operations CMP‡ method			
Chisel	–	45.3 ± 13.1	158.9 ± 140.1***	69.0 ± 19.9***	278.0	265.9 ± 76.6
Optimizer	71.2 ± 109.6***	32.5 ± 5.1***	103.5 ± 121.0***	42.7 ± 6.6***	385.4	169.9 ± 26.2
Sum	–	77.8 ± 14.0	262.4 ± 185.1***	111.6 ± 20.9***	663.4	435.8 ± 80.9
			Conventional method			
Disc 1	–	20.4 ± 2.6	125.6 ± 57.9***	99.7 ± 12.5***	1018.2	159.8 ± 20.0
Chisel	34.5 ± 115.1 ns§	35.8 ± 5.9 ns	167.5	79.5 ± 13.1	423.2	235.1 ± 38.8
Disc 2	23.3 ± 7.4***	39.5 ± 11.2***	149.2 ± 91.8***	80.7 ± 20.5***	1210.0	149.3 ± 40.3
Land plane	18.4	13.8 ± 3.9	41.3 ± 10.6***	21.9 ± 6.2***	38.9	33.4 ± 9.4
Sum	–	109.5 ± 13.5	483.6	281.9 ± 28.0	2690.2	577.6 ± 60.1
			Control effectiveness			
			%			
η ± 1σ	–	28.9 ± 1.6	45.7	60.4 ± 0.7	75.3	24.6 ± 1.3

*** Differences between emission calculation methods is significant at the 0.001 probability level.

† EF, emission factor; LIDAR, light detection and ranging; $PM_{2.5}$, particulate matter with an equivalent aerodynamic diameter ≤2.5 μm; PM_{10}, particulate matter with an equivalent aerodynamic diameter ≤10 μm; TSP, total suspended particulate (particulate matter with an equivalent aerodynamic diameter ≤100 μm).

‡ Conservation management practice

§ Nonsignificant at the 0.20 probability level.

based on the number of total valid downwind scans collected each day.

The lowest EF among the investigated operations for each PM size fraction and EF calculation methodology was derived for the land plane operation in the conventional tillage method. Emission factors available in literature for land planning are generally higher than all other activities by a factor of 10. This relationship between the EF for land planing and discing/tilling/chiseling was not seen in this study. The much lower EFs for land planing are likely due to the water remaining in the soil surface from the precipitation event that occurred 2 d prior, as calculated from downwind latent heat measurements.

Statistical comparisons between the mean reported ERs and EFs from the two emission estimation techniques and within a PM size fraction and operation were made via independent t tests for all pairs in which $n > 2$ for the inverse modeling technique (i.e., all pairs reporting CIs about both average values). The results are presented in Tables 4 and 5, showing that the differences between all but one pair of averages with sufficient data points were statistically significant at the 0.001 probability level. The difference between the lone pair was found not to be significant at the 0.20 probability level. Only one instance of tillage method sums with sufficient inverse modeling data points to perform an independent t test exists in this dataset, the combined operations CMP method for the PM_{10} size fraction; the differences between the summed emissions for the two techniques were found to be statistically significant at the 0.001 probability level. For those pairs without sufficiently large n for the inverse modeling technique to report a confidence interval, a more qualitative comparison may be made between the inverse modeling estimates with the average LIDAR values ±95% CI. In the majority of such cases, the estimated inverse modeling value was greater than the average LIDAR-based emission value plus the 95% CI, a pattern present throughout the dataset. This pattern of higher inverse modeling emissions estimates than LIDAR estimates is similar to the findings of Marchant et al. (2011), who investigated PM emissions from a dairy using inverse modeling with AERMOD and mass balance applied to LIDAR data.

Although inverse modeling emissions are usually a factor of two to three higher, two inverse modeling TSP ERs and EFs are significantly higher by factors of six (disc 1 operation) and eight (disc 2 operation). These large differences in the two disc operation EFs lead to a much larger difference between emission estimation techniques in TSP EF sums for the conventional tillage method than for the combined operations CMP method, which in turn cause a large difference in calculated TSP control efficiencies between emission calculation methodologies. In addition, ERs across tillage operations for a given PM fraction and ER calculation method do not generally vary by more than a factor of

three, with the exception of the land plane TSP ER estimated through inverse modeling. The ERs measured and reported for the Optimizer pass of the combined operation CMP are among the higher values for each PM fraction herein reported, though they are not always the highest. When the total tractor time is accounted for in the EF calculation, the Optimizer emissions move toward the lower end of the measured EF values due to the tillage rate being approximately twice that of the other operations (Table 1).

Methodology limitations may contribute to the differences observed between reported ERs and EFs. First, the LIDAR was unable to monitor plumes below 8 m agl in this test due to laser safety concerns and may have thus underestimated emissions due to the unmeasured PM leaving the field below 8 m agl. Second, the ability of the model to simulate observed vertical dispersion appears to have been limited in some cases, as demonstrated in Fig. 2. These images compare average PM_{10} concentrations along the vertical downwind LIDAR scanning plane as calculated from LIDAR return signal for the 23 October measurement period and as predicted by AERMOD using the LIDAR-derived PM_{10} ER from the same period. Although the model predicts PM levels decreasing exponentially with height, the LIDAR detected significant PM above 50 m agl. The highest concentrations in some plumes
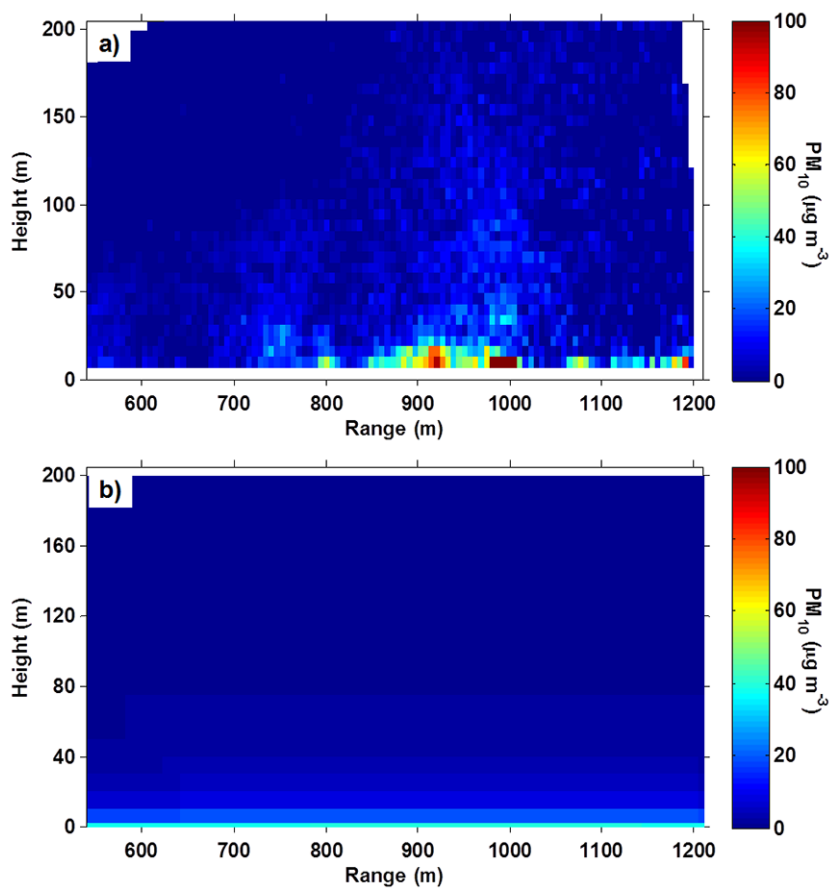

Fig. 2. Period-averaged particulate matter with an equivalent aerodynamic diameter ≤10 μm (PM_{10}) concentrations (μg m⁻³) resulting from the tillage activity on 23 October along the vertical downwind lidar scanning plane as (a) estimated by light detection and ranging (LIDAR) (average downwind minus average upwind) and (b) predicted by The American Meteorological Society and USEPA regulatory model (AERMOD) using the LIDAR-derived emission rate for this sample period. The minimum elevation measurement of the LIDAR was 8 m due to safety concerns.

were measured far above the surface (Fig. 3). This limited simulation of observed vertical dispersion decreases predicted concentrations relative to the actual measured impact at elevations above the release height, leading to higher inverse modeling estimated emissions to better match the elevated MiniVol measurements.

The PM_{10} EFs for conventional tillage operations estimated during this study are occasionally in agreement with values reported by Flocchini et al. (2001), Kasumba et al. (2011), Madden et al. (2008), and Wang et al. (2010) and those given by the California ARB (2003a). Although the values from all the previously published studies are generally not in close agreement, they are within the range of the variability expected from measurements made under different meteorological and soil conditions, as demonstrated by the wide range of values from Flocchini et al. (2001).

The EFs for each tillage method were quantified to compare the control effectiveness (η) of the CMP as calculated from the following equation based on the approach described by Cooper and Alley (2002).

$$\eta = \frac{EF_{CT} - EF_{COT}}{EF_{CT}}$$

where EF_{CT} is the summed EF for the conventional tillage method, and EF_{COT} is the summed EF for the combined operations tillage method. Calculated values of η are listed in Table 5 for each size fraction. The lack of a complete $PM_{2.5}$ EF dataset from the inverse modeling method prevents this comparison, and the singular TSP data point for each operation in the same method excludes statistical measure estimates. However, emissions values based on LIDAR data are complete and were therefore used to represent the CMP control efficiency for all size fractions. The particulate emissions control efficiency of the combined operations CMP ± 1σ, as monitored by LIDAR in this study, were 29 ± 2%, 60 ± 1%, and 25 ± 1% for $PM_{2.5}$, PM_{10}, and TSP, respectively.

Another important result of this investigation is the assessment of the utility of LIDAR for measuring and AERMOD for simulating particulate emissions in an agricultural setting. These LIDAR measurements clearly indicate that LIDAR is an effective tool for visualizing plumes from tillage operations. When mass calibrated, it functions as a virtual broad array of fast response point samplers. Specifically, the LIDAR captured far more particulate matter suspended at heights above 20 m than AERMOD predicts (Fig. 2). This poses larger questions about the role of PM entrainment and transport away from the tillage site, a question that is beyond the scope of this manuscript. Also, it is difficult to accurately simulate the emission characteristics from these tillage studies with AERMOD because it is being used at the limit of its designed performance. The analysis of the emissions between the two methods differs in that a point sampler–based model uses a mathematical function to estimate plume characteristics based on a handful of data points, whereas the LIDAR directly sums the results from all bins to determine the extent and concentration of the plume and the strength of the source. It is clear that the incorporation of LIDAR measurements
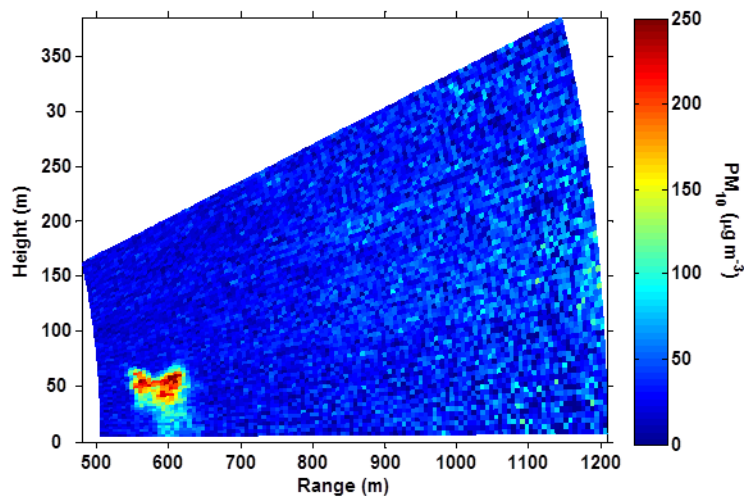

Fig. 3. Light detection and ranging (LIDAR)-measured downwind particulate matter with an equivalent aerodynamic diameter ≤10 μm (PM_{10}) concentrations (μg m^{-3}) from a single vertical scan on 23 October. A tillage plume is seen crossing the LIDAR scan at a range of 600 m and centered at 50 m above ground level. The minimum elevation measurement of the LIDAR was 8 m due to safety concerns.

is an important complement to ground-based sensors because ground-based sensors cannot measure elevated plumes.

Conclusions

Aerosol concentrations resulting from traditional agricultural tillage activities and the combined operations CMP were successfully measured with point sensors and a mass-calibrated, scanning LIDAR system. Emission rates and EFs for TSP, PM_{10}, and $PM_{2.5}$ were calculated based on point and the remote sensor datasets to quantify the control effectiveness of the CMP. These EFs were generally in agreement with and within the variability of those found in the literature, except for the EFs estimated for the land plane operation. The estimated emissions from the inverse modeling methodology were usually higher than those calculated from LIDAR data; most differences between the two techniques were statistically significant where a statistical comparison was possible. The CMP control effectiveness per PM size fraction was estimated based on LIDAR-derived ERs due to dataset completeness. The control effectiveness values ±1σ were 29 ± 2%, 60 ± 1%, and 25 ± 1% for $PM_{2.5}$, PM_{10}, and TSP, respectively.

The mass-calibrated LIDAR proved very effective in detecting downwind plumes and, in combination with wind vector and upwind PM measurements, quantifying dust emissions from the tillage activities. Downwind plumes of significant concentration were frequently detected by Aglite at elevations much greater than that predicted by AERMOD, even up to 200 m. This suggests that application of such air dispersion models to activities similar in spatial and temporal variability to agricultural tillage should be done carefully and conservatively.

References

Arya, S.P. 1998. Air pollution meteorology and dispersion. Oxford Univ. Press, New York.

Bingham, G.E., C.C. Marchant, V.V. Zavyalov, D.J. Ahlstrom, K.D. Moore, D.S. Jones, et al. 2009. Lidar based emissions measurement at the whole facility scale: Method and error analysis. J. Appl. Remote Sens. 3(1):033510. doi:10.1117/1.3097919

California ARB. 2003a. Area source methods manual, section 7.4: Agricultural land preparation. California Air Resources Board. www.arb.ca.gov/ei/areasrc/fullpdf/full7-4.pdf (accessed 7 Nov. 2011).

California ARB. 2003b. Area source methods manual, section 7.5: Agricultural harvest operations. California ARB. www.arb.ca.gov/ei/areasrc/fullpdf/full7-5.pdf (accessed 7 Nov. 2011).

Cooper, D.C., and F.C. Alley. 2002. Air pollution control: A design approach. 3rd ed. Waveland Press Inc., Prospect Heights, IL.

Doran, J.W., and A.J. Jones. 1996. Methods for assessing soil quality. SSSA Special Publication 49. SSSA, Madison, WI.

Flocchini, R.G., T.A. James, L.L. Ashbaugh, M.S. Brown, O.F. Carvacho, B.A. Holmen, et al. 2001. Interim report: Sources and sinks of PM_{10} in the San Joaquin Valley. Crocker Nuclear Laboratory, UC–Davis, CA. www.arb.ca.gov/research/apr/reports/l2022.pdf (accessed 7 Nov. 2011).

Holmen, B.A., W.E. Eichinger, and R.G. Flocchini. 1998. Application of elastic LIDAR to PM_{10} emissions from agricultural nonpoint sources. Environ. Sci. Technol. 32:3068–3076. doi:10.1021/es980176p

Holmen, B.A., T.A. James, J.L. Ashbaugh, and R.G. Flocchini. 2001a. LIDAR-assisted measurement of PM_{10} emissions from agricultural tilling in California's San Joaquin Valley—Part I. LIDAR. Atmos. Environ. 35:3251–3264. doi:10.1016/S1352-2310(00)00518-5

Holmen, B.A., T.A. James, J.L. Ashbaugh, and R.G. Flocchini. 2001b. LIDAR-assisted measurement of PM_{10} emissions from agricultural tilling in California's San Joaquin Valley—Part II: Emission factors. Atmos. Environ. 35:3265–3277. doi:10.1016/S1352-2310(00)00519-7

Kasumba, J., B.A. Holmen, A. Hiscox, J. Wang, and D. Miller. 2011. Agricultural PM10 emissions from cotton field disking in Las Cruces, NM. Atmos. Environ. 45:1668–1674. doi:10.1016/j.atmosenv.2011.01.004

Madden, N.M., R.J. Southard, and J.P. Mitchell. 2008. Conservation tillage reduces PM10 emissions in dairy forage rotations. Atmos. Environ. 42:3795–3808. doi:10.1016/j.atmosenv.2007.12.058

Marchant, C.C., T.D. Wilkerson, G.E. Bingham, V.V. Zavyalov, J.M. Andersen, C.B. Wright, et al. 2009. Aglite lidar: A portable elastic lidar system for investigating aerosol and wind motions at or around agricultural production facilities. J. Appl. Remote Sens. 3(1):033511. doi:10.1117/1.3097928

Marchant, C.C., K.D. Moore, M.D. Wojcik, R.S. Martin, R.L. Pfeiffer, J.H. Prueger, et al. 2011. Estimation of dairy particulate matter emission rates by lidar and inverse modeling. Trans. ASABE 54:1453–1463.

San Joaquin Valley Air Pollution Control District (SJVAPCD). 2006. Conservation management practices program report for 2005. San Joaquin Valley Air Pollution Control District, Fresno, CA. http://www.valleyair.org/farmpermits/updates/cmp_program_report_for_2005.pdf (accessed 7 Nov. 2011).

Soil Survey Staff. 2007. Web soil survey 2.0. USDA–NRCS. http://websoilsurvey.nrcs.usda.gov/app/ (accessed 2 Oct. 2007).

USEPA. 1987. 40 CFR Appendix J to Part 50: Reference method for the determination of particulate matter as PM10 in the atmosphere. Fed. Regist. 54:24664.

Wang, J., D.R. Miller, T.W. Sammis, A.L. Hiscox, W. Yang, and B.A. Holmen. 2010. Local dust emission factors for agricultural tilling operations. Soil Sci. 175(4):194–200. doi:10.1097/SS.0b013e3181dae283

Williams, D.J., S. Chilingaryan, and J. Hatfield. 2012. Los Banos, CA Fall 2007 Tillage Campaign: Data analysis. USEPA Rep. EPA/600/R-12/734. U.S. Gov. Print. Office, Washington, DC. http://cfpub.epa.gov/si/si_public_record_report.cfm?dirEntryId=248752 (accessed 1 Mar. 2013).

Zavyalov, V.V., C.C. Marchant, G.E. Bingham, T.D. Wilkerson, J.L. Hatfield, R.S. Martin, et al. 2009. Aglite lidar: Calibration and retrievals of well characterized aerosols from agricultural operations using a three-wavelength elastic lidar. J. Appl. Remote Sens. 3(1):033522. doi:10.1117/1.3122363